

Lateral manipulation with combined atomic force and scanning tunneling microscopy using CO-terminated tips

Julian Berwanger,* Ferdinand Huber, Fabian Stilp, and Franz J. Giessibl

Institute of Experimental and Applied Physics, University of Regensburg, 93053 Regensburg, Germany

(Dated: July 23, 2022)

CO-terminated tips currently provide the best spatial resolution obtainable in atomic force microscopy. Due to their chemical inertness, they allow to probe interactions dominated by Pauli repulsion. The small size and inertness of the oxygen front atom yields unprecedented resolution of organic molecules, metal clusters and surfaces. However, CO tips are flexible laterally and evidence that they can be used for lateral manipulation experiments has been missing. We study the capability of CO-terminated tips to laterally manipulate single iron adatoms on the Cu(111) surface with combined atomic force and scanning tunneling microscopy at 7 K. Furthermore, we find that even a slight asymmetry of the tip results in a distortion of the lateral force field. In addition, the influence of the tilt of the CO tip on the lateral force field is inverted compared to the use of a monoatomic metal tip which we can attribute to the inverted dipole moment of a CO tip with respect to a metal tip. Moreover, we demonstrate atom-by-atom assembly of iron clusters with CO tips while using the high resolution capability of the CO tips in between to determine the arrangement of the individual iron atoms within the cluster. Finally, we are able to manipulate single copper and silicon adatoms laterally and, additionally, create a silicon cluster by lateral manipulation without changing or losing the CO-terminated tip.

Since Eigler and Schweizer performed the very first atomic positioning experiments with individual xenon atoms on Ni(110) by using a scanning tunneling microscope [1], atomic manipulation became a widely used technique in the field of scanning probe microscopy [2–6]. It was found that lateral manipulation processes can occur due to repulsion (pushing) where the atom is moving away from the tip, attraction (pulling) where the atom is manipulated towards the tip or in a continuous mode (sliding) where the atom is trapped in the force field of the tip [3]. Ternes *et al.* [7] were the first to probe atomic forces acting during the manipulation process by using non-contact atomic force microscopy (nc-AFM) [8]. Lateral manipulation was used for building up logical operators [9] and nano magnets consisting of a single digit count of magnetic iron atoms while the exact geometric adsorption of the built iron structures remained unclear, due to lack of structural high-resolution capabilities of metal tips [10, 11]. Bartels *et al.* [12] proposed the transfer of a carbon monoxide (CO) molecule to the apex of a metal tip which revealed for the first time intramolecular resolution in AFM [13] and later atomic resolution of small metal clusters [14], and is now a standard method in high resolution AFM [15, 16]. It was shown that CO-terminated tips (CO tips) yield, especially on molecules, a higher atomic contrast compared to other tip functionalizations [17]. The usage of CO tips including the handling of bending effects in the acquired images are well established and the exact imaging mechanism has been extensively studied in theory and experiment [18–23]. However, the combination of high-resolution imaging and lateral manipulation has been lacking so far. Combining both allows for example to build atomic clusters with a predetermined structure while the CO tip can be used for imaging and lateral

manipulation at the same time. This combination is more efficient compared to the common technique of using metal tips for the manipulation process and CO tips for imaging, especially, if the manipulation and imaging cycle will be repeated several times.

In this Letter, we study the manipulation of single iron adatoms using CO tips and compare it to lateral manipulation performed with commonly-used metal tips. Furthermore, we investigate the influence of the tilt of the tips on the experiment. Additionally, we build up iron clusters atom by atom using CO tips and use the high-resolution capability of the CO tips to resolve the atomic arrangement of the clusters in between. We demonstrate that reproducible lateral manipulation with CO tips is possible without changing or losing the CO tip during these experiments.

All experiments were performed with a custom-built combined atomic force and scanning tunneling microscope at 7 K equipped with a qPlus sensor [24] ($k = 1800 \text{ N/m}$, $f_0 = 26447.5 \text{ Hz}$, $Q = 163249$) operating in frequency-modulation mode [8]. To maximize sensitivity to short-range forces, an amplitude of 50 pm was chosen [25]. An electrochemically etched tungsten wire was used as a tip which was poked repeatedly into the clean Cu(111) sample in order to generate a monoatomic metal tip. To confirm this, we performed the carbon monoxide front atom identification (COFI) method [26]. For this, less than 0.01 monolayers of CO were dosed onto the surface and the tip was scanned in constant height above a single CO molecule. The CO molecule on the surface acts effectively as a probe which images the AFM tip and reveals its geometrical structure in the frequency shift Δf image [14]. The monoatomic metal tip was functionalized with a CO molecule [12]. By using such tips, the hexagonal Cu(111) surface lattice

with fcc and hcp hollow sites was resolved in the Δf channel [4, 12]. Single iron atoms were evaporated onto the cold Cu(111) surface which adsorb in fcc hollow sites [27, 28]. Each individual iron adatom is surrounded by six equivalent next-neighbor fcc hollow sites on the surface (see inset in Fig. 1(a)). The lateral manipulation experiments were performed with various monoatomic metal and CO tips along the six high-symmetry directions $\vec{x} \in \{\pm\vec{x}_A, \pm\vec{x}_B, \pm\vec{x}_C\}$. The initial tip-sample distance z_{start} was chosen large enough to start with a flat $\Delta f(x, z_{\text{start}})$ profile. Beginning from z_{start} , consecutive linescans over the iron adatom were performed while reducing the tip-sample distance by 5 pm after each linescan. To make sure that the adatom is only manipulated in the forward direction, the tip was retracted by 50 pm when moving backwards. To isolate the interaction between tip and adatom, the frequency shift above the Cu(111) surface is subtracted from each $\Delta f(x, z)$ curve. Afterwards, the short-range potential U_{SR} between tip and adatom was deconvoluted [29, 30] and, by lateral differentiation, the lateral force $F_{x,\text{SR}}(x, z) = -\partial U_{\text{SR}}(x, z)/\partial x$ acting between tip and adatom was determined (for further experimental details see SP1 and SP2 in the Supplemental Material [31]).

Figure 1(a) shows selected $\Delta f(x)$ linescans acquired with a monoatomic metal tip along the \vec{x}_A -direction. The iron adatom is located at $x_A = 0$ pm. At $z_{\text{start}} = z_1$, the $\Delta f(x_A)$ curve is flat. The $\Delta f(x_A, z_2)$ linescan shows an attractive dip centered at the iron adatom. The closer the tip approaches the surface the deeper the dip above the iron atom evolves. In the lowest curve, a sharp change in the Δf signal, indicated by the vertical green dotted line at $x_A = x_{\text{man}}$ can be observed after the tip has passed the center of the iron adatom. After that, the iron atom is imaged at its new lateral position at $x_A = 255$ pm (see Fig. S2 [31]). The change in x_A of 255 pm corresponds to the next-neighbor distance of the Cu(111) surface [32]. Hence, the iron atom was manipulated laterally to the next-neighbor fcc hollow site along the positive \vec{x}_A -direction (to the right side). Next, the very same metal tip was functionalized with a CO molecule and the experiment was repeated (see Fig. 1(b)). Curve 2 shows a single attractive dip above the iron adatom. Getting closer results in an evolution of two bumps next to the center, besides of the attractive dip at the center of the iron adatom. In the x - y -plane, these bumps yield a torus which was observed in previous experiments [14] (see inset Fig. 3(a)). At the closest tip-sample distance, a sharp change in the Δf curve at $x_A = x'_{\text{man}}$ occurs before the tip has passed the center of the iron adatom. Here, the iron adatom is manipulated by one lattice position along the negative \vec{x}_A -direction (to the left side).

The lateral force curves of the interaction between metal tip and iron adatom and between CO tip and iron adatom, respectively, derived from the deconvoluted

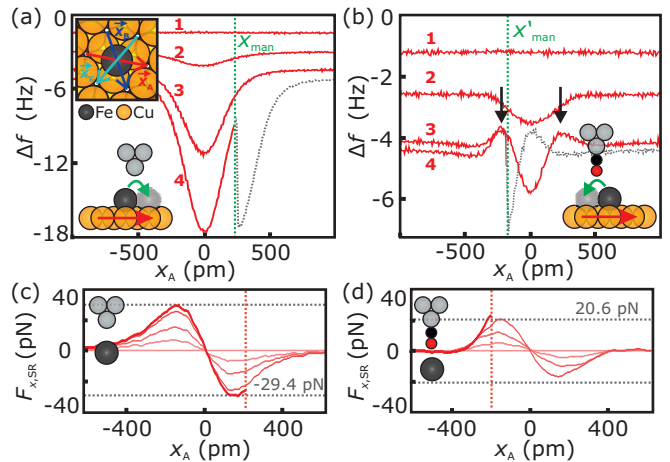


FIG. 1. (a) Selected raw $\Delta f(x_A, z_i)$ traces ($z_1 = 571$ pm, $z_2 = 291$ pm, $z_3 = 211$ pm, $z_4 = 186$ pm) acquired with a monoatomic metal tip along the \vec{x}_A -direction are shown. The z values refer to the distances to point contact on the Cu(111) surface [7, 31, 33]. $x_A = 0$ pm indicates the center of the iron adatom before manipulation. It is manipulated at $x_{\text{man}} > 0$ pm, indicated by the green dotted line. The grey dotted trace is the $\Delta f(x_A)$ curve after manipulation. The inset shows a sketch of a Cu(111) surface with an iron adatom adsorbed on a fcc hollow site in top-view. The vectors \vec{x}_A , \vec{x}_B and \vec{x}_C indicate the directions to three next-neighbor fcc hollow sites. Panel (b) depicts selected $\Delta f(x_A, z_i)$ curves ($z_1 = 560$ pm, $z_2 = 340$ pm, $z_3 = 220$ pm, $z_4 = 205$ pm) by using a CO tip. In this case, the iron adatom is manipulated before the tip has crossed the center of the adatom at $x_{\text{man}} < 0$ pm. The complete $\Delta f(x_A)$ data sets of panels (a) and (b) are shown in Fig. S3 [31]. Panels (c) and (d) show selected lines of the corresponding lateral force $F_{x,\text{SR}}(x_A)$. Darker lines refer to closer tip-sample distances. The absolute lateral force increases with decreasing tip-sample distance z . Before the deconvolution processes, a Gaussian filter ($\sigma = 16$ pm) was applied on the Δf data.

short-range potential $U_{\text{SR}}(x_A, z)$ (see Fig. S4 [31]), are qualitatively quite similar (Figs. 1(c) and (d)). The sign of the force value indicates whether the force acting on the adatom points to the left (+) or right direction (-). Hence, in both cases, the lateral forces acting between tip and adatom are attractive. As the tip approaches the center of the iron adatom from the left side, a positive lateral force acts on the adatom which points to the left side (towards the tip). After the tip has passed the center at $x_A = 0$ pm, a negative lateral force acts on the adatom, which points to the right side. As only attractive interactions are observed, the actual manipulation of iron adatoms, using monoatomic metal and CO tips, is a pulling process [3]. In case of the monoatomic metal tip, the absolute values of the lateral forces are about 1% higher for $x_A > 0$ pm compared to $x_A < 0$ pm and, therefore, the iron adatom is manipulated laterally after the tip has passed the center of the adatom (red dotted vertical line in Fig. 1(c)), since

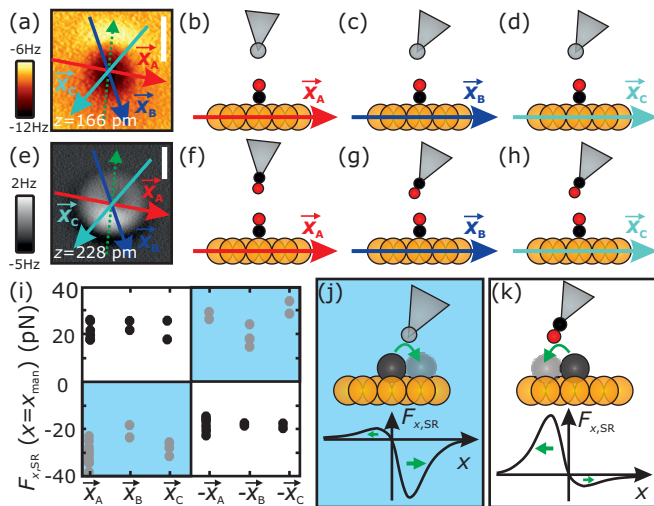


FIG. 2. (a) Constant-height Δf image acquired above a CO molecule (COFI image) shows a tilted monoatomic metal tip [26, 34]. The scale bar length is 300 pm. Panels (b)-(d) depict the tilt of the monoatomic metal tip along the three high-symmetry directions of the Cu(111) surface. Panel (e) displays the COFI image of the very same metal tip from (a) with a CO molecule attached to its apex. Due to symmetry reasons, the CO molecule adsorbs to the tip's apex as illustrated in panels (f)-(h) for the three high-symmetry direction of Cu(111). (i) Lateral force acting at the moment of manipulation against manipulation direction. The tilt of the tips introduces an asymmetry in the force profiles. In case of the monoatomic metal tip, the iron adatom is at first manipulated when the tilted part of the tip is facing away from the adatom (as sketched in panel (j)). For CO tips, the initial lateral manipulation of the iron adatom takes place when the tilted part of the tip is facing towards the adatom (as sketched in panel (k)).

the force threshold [7, 34] for lateral manipulation is overcome the first time. The manipulation of the iron adatom with the same metal tip from Fig. 1(c) but terminated with a CO leads to an inverted asymmetry: The lateral forces before crossing the iron adatom are by about 10% higher than after crossing the adatom (see horizontal grey dotted lines in Fig. 1(d)). Hence, the iron adatom is already manipulated before the tip was passing. A further analysis of the exact movement of the iron adatom is described in SP6 [31].

To further investigate this asymmetry, the manipulation experiment was performed in all six high-symmetry directions of Cu(111) and the COFI images of the monoatomic metal and CO tip are analyzed in detail. Figure 2(a) shows the COFI image ($\Delta f(x, y)$) of the monoatomic metal tip. The image reveals a tilt of the tip whose direction can be determined by investigating the repulsive (bright) sickle in the top part of the image [26, 34]. This sickle is present because the tilted part of the tip at these (x, y) positions is closer to the CO molecule and the interaction in the repulsive

regime compared to the positions mirrored at the center of the CO molecule. To clarify this, the tilt of the metal tip is sketched in Figs. 2(b)-(d) for the high-symmetry manipulation directions. The \vec{x}_A -direction is almost perpendicular to the symmetry axis of the tip (see dashed arrow in Fig. 2(a)) and, therefore, the $F_{x,SR}(x_A)$ curves in Fig. 1(c) show only a slight asymmetry with respect to $x_A = 0$ pm. Along the \vec{x}_B - and \vec{x}_C -directions, the tilt of the tip is more significant and, hence, also the lateral force profiles are more asymmetric (see $F_{x,SR}(x_B)$ in Fig. S5 [31]). Figure 2(e) shows the COFI image of the monoatomic metal tip from Fig. 2(a) with a CO molecule attached to its apex. Due to symmetry reasons, the CO molecule adsorbs to the tip's apex as sketched in Figs. 2(f)-(h). This suggestion is supported by the observation of the attractive sickle in the bottom part of the image (for a deeper analysis regarding the tilt determination see SP10 and SP11 [31]).

Figure 2(i) depicts the lateral forces acting in the moment of lateral manipulation with respect to the manipulation direction \vec{x} . Grey colored data points correspond to manipulation experiments with two monoatomic metal tips whereas black data points result from experiments with three different CO functionalized tips. As discussed before, positive or negative force values indicate whether the iron adatom is manipulated before or after the tip has passed the center of the iron adatom, respectively. Although the metal tip and the CO tip are tilted in similar directions, the influence of the tilt onto the initial manipulation direction is inverted: For monoatomic metal tips, the lateral forces are always higher in absolute value when the tilted part of the tip is facing away from the adatom, as sketched in Fig. 2(j), and, therefore, the manipulation occurs at first when the tilted part of the tip is facing away from the adatom. Hence, the forces in Fig. 2(i) are negative for $\vec{x} \in \{\vec{x}_A, \vec{x}_B, \vec{x}_C\}$ and positive for $\vec{x} \in \{-\vec{x}_A, -\vec{x}_B, -\vec{x}_C\}$. Contrary behavior is observed for the manipulation with CO tips: The absolute value of the lateral forces shows a maximum when the tilted part of the tip is facing the adatom, as sketched in Fig. 2(k) and, thus, the lateral forces are positive for $\vec{x} \in \{\vec{x}_A, \vec{x}_B, \vec{x}_C\}$ and negative for $\vec{x} \in \{-\vec{x}_A, -\vec{x}_B, -\vec{x}_C\}$, respectively. Therefore, attaching a CO molecule to a monoatomic metal tip inverts the influence on the asymmetry in the lateral force profile. As a consequence, a metal tip oriented as in Fig. 2(j) needs to be closer to the surface for a manipulation to the left than for a manipulation to the right and vice-versa for a CO tip like in Fig. 2(k).

To investigate the reason for this inversion, we applied an analytic model considering van der Waals [35] and electrostatic [36] interactions between a tilted tip and an iron atom. The important difference between a CO tip and a metal tip is the direction of their dipole moment: The Smoluchowski effect [37] leads to a positive dipole of the metal tip while a CO tip obtains a negative dipole

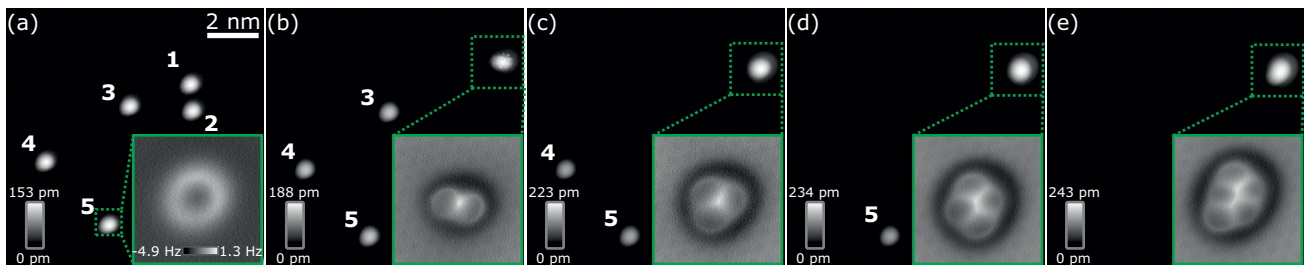


FIG. 3. Panels (a) through (e) show topographic images of the same area acquired in constant-current mode ($V_{\text{tip}} = -10$ mV, $\langle I \rangle = 10$ pA). By performing controlled lateral manipulation using a CO tip, a cluster consisting of five individual iron adatoms is formed atom by atom. The cluster is imaged after each lateral manipulation event with a higher current setpoint in order to obtain atomic resolution within the cluster. The insets of each panel depict the Δf image acquired in (a) constant-height mode and (b)-(e) constant-current mode, respectively ($V_{\text{tip}} = -10$ mV, $\langle I \rangle = 300$ pA, same colorscales).

[22, 33]. In our simulations, the inverted dipole moment causes, in the close distance regime, the asymmetry of the lateral force field as sketched in Figs. 2(j) and (k) (see SP12 [31] for the simulation and further information).

The average lateral force threshold needed for lateral manipulation of an iron adatom on Cu(111) using monoatomic metal tips is 27 ± 6 pN which is comparable to the value that holds for CO tips (20 ± 4 pN). Moreover, our determined force values are similar to the lateral force value needed to manipulate a cobalt adatom laterally with an uncharacterized metal tip on the Cu(111) surface (17 ± 3 pN) [7]. However, Negulyaev *et al.* experimentally found a diffusion barrier of 22 ± 7 meV for iron adatoms on Cu(111) which matches their calculated diffusion barrier of 28.5 meV [28]. By using a sinusoidal model potential, this translates into a lateral force needed to overcome these barriers of 65 ± 20 pN and 84.4 pN, respectively. Emmrich *et al.* [34] proposed a lowering of the potential barrier by 50% due to the presence of the AFM tip in lateral manipulation experiments of single CO molecules on Cu(111). In our experiments with single iron adatoms on Cu(111), the lowering of the potential barrier is up to 70% with respect to the theoretical value of 28.5 meV [28], and, hence, even higher.

In order to investigate the stability of CO tips regarding lateral manipulation further, we built up iron clusters atom by atom using a CO tip. Figure 3(a) shows a topographic image of five individual iron atoms adsorbed on Cu(111). The constant-height Δf image resolves the toroidal structure [14] of a single adatom (see inset of Fig. 3(a)). Afterwards, the adatoms 1 and 2 were pulled together via lateral manipulation (see topographic image in Fig. 3(b)). The CO tip directly allows to resolve the individual atoms within the formed dimer in Δf (see inset Fig. 3 (b)). Figures 3(c) through (e) depict the same scan frame after adding one after the other atom to the cluster. The inset of Fig. 3(e) depicts the internal structure of the created pentamer. We

artificially constructed five pentamers with various CO tips (see Fig. S14 [31]) and find that the atoms arrange always in-plane which answers the question raised by Khajetoorians *et al.* [11] about the exact arrangement of magnetic iron pentamers. The tunneling current and Δf versus distance spectra acquired on a CO molecule before and after the cluster construction are identical which proves that the CO tip didn't change during the experiment (see Fig. S15 [31]). Additionally, we conducted sliding experiments with CO tips. Sliding is possible if the lateral force threshold for lateral manipulation for tip positions $x < 0$ pm and $x > 0$ pm is overcome and the adatom is trapped inside the force field of the tip. By moving the tip laterally, single iron, copper and silicon adatoms can be slid over the substrate without changing or losing the CO tip. Furthermore, we were able to create a silicon trimer out of three single silicon adatoms by lateral manipulation with a CO tip (see Fig. S16 [31]).

We conclude that lateral manipulation of single iron adatoms on Cu(111) with CO tips and monoatomic metal tips occur both in an attractive pulling mode. Furthermore, we find that a slight tilt of the tip causes an asymmetry of the lateral force profiles which results in an atomic ratchet: At a particular tip-sample distance, lateral manipulation of single iron adatoms is only possible in one direction while the direction is opposite using CO tips with respect to monoatomic metal tips. We can explain the inverted influence of tilted CO tips on the asymmetry of the lateral force field by the inverted dipole of the tips. Moreover, we find that by approaching the CO tip further, single iron, copper and silicon adatom can be slid continuously over the Cu(111) surface. Finally, we show that atom-by-atom assembly of iron clusters via lateral manipulation using CO tips is possible while the high-resolution capability of CO tips can be used for determining the geometric structure of the clusters. In all experiments, the manipulation was possible without losing the CO from the tip's apex.

The authors thank N. Hauptmann and A. J. Weymouth for fruitful discussions and the Deutsche Forschungsgemeinschaft for funding within the research Projects No. SFB 689, project A9 and CRC 1277, project A02.

* julian.berwanger@ur.de

- [1] D. M. Eigler and E. K. Schweizer, *Nature* **344**, 524 (1990).
- [2] J. A. Stroscio and D. M. Eigler, *Science* **254**, 1319 (1991).
- [3] L. Bartels, G. Meyer, and K.-H. Rieder, *Physical Review Letters* **79**, 697 (1997).
- [4] J. A. Stroscio and R. J. Celotta, *Science* **306**, 242 (2004).
- [5] R. J. Celotta, S. B. Balakirsky, A. P. Fein, F. M. Hess, G. M. Rutter, and J. A. Stroscio, *Review of Scientific Instruments* **85**, 121301 (2014).
- [6] F. E. Kalf, M. P. Rebergen, E. Fahrenfort, J. Girovsky, R. Toskovic, J. L. Lado, J. Fernández-Rossier, and A. F. Otte, *Nature Nanotechnology* **11**, 926 (2016).
- [7] M. Ternes, C. P. Lutz, C. F. Hirjibehedin, F. J. Giessibl, and A. J. Heinrich, *Science* **319**, 1066 (2008).
- [8] T. R. Albrecht, P. Grütter, D. Horne, and D. Rugar, *Journal of Applied Physics* **69**, 668 (1991).
- [9] A. A. Khajetoorians, J. Wiebe, B. Chilian, and R. Wiesendanger, *Science* **332**, 1062 (2011).
- [10] A. A. Khajetoorians, J. Wiebe, B. Chilian, S. Lounis, S. Blügel, and R. Wiesendanger, *Nature Physics* **8**, 497 (2012).
- [11] A. A. Khajetoorians, B. Baxevanis, C. Hubner, T. Schlenk, S. Krause, T. O. Wehling, S. Lounis, A. Lichtenstein, D. Pfannkuche, J. Wiebe, and R. Wiesendanger, *Science* **339**, 55 (2013).
- [12] L. Bartels, G. Meyer, and K.-H. Rieder, *Applied Physics Letters* **71**, 213 (1997).
- [13] L. Gross, F. Mohn, N. Moll, P. Liljeroth, and G. Meyer, *Science* **325**, 1110 (2009).
- [14] M. Emmrich, F. Huber, F. Pielmeier, J. Welker, T. Hofmann, M. Schneiderbauer, D. Meuer, S. Polesya, S. Mankovsky, D. Ködderitzsch, H. Ebert, and F. J. Giessibl, *Science* **348**, 308 (2015).
- [15] N. Pavliček and L. Gross, *Nature Reviews Chemistry* **1**, 0005 (2017).
- [16] A. Extnance, *Nature* **555**, 545 (2018).
- [17] F. Mohn, B. Schuler, L. Gross, and G. Meyer, *Applied Physics Letters* **102**, 073109 (2013).
- [18] N. Moll, L. Gross, F. Mohn, A. Curioni, and G. Meyer, *New Journal of Physics* **12**, 125020 (2010).
- [19] M. Neu, N. Moll, L. Gross, G. Meyer, F. J. Giessibl, and J. Repp, *Physical Review B* **89**, 205407 (2014).
- [20] P. Hapala, G. Kichin, C. Wagner, F. S. Tautz, R. Temirov, and P. Jelinek, *Physical Review B* **90**, 085421 (2014).
- [21] P. Hapala, M. Svec, O. Stetsovych, M. Ondracek, P. Mutoombo, P. Jelinek, J. van der Lit, N. J. van der Heijden, and I. Swart, *Nature Communications* **7**, 11560 (2016).
- [22] M. Ellner, N. Pavliček, P. Pou, B. Schuler, N. Moll, G. Meyer, L. Gross, and R. Pérez, *Nano Letters* **16**, 1974 (2016).
- [23] J. van der Lit, F. Di Cicco, P. Hapala, P. Jelinek, and I. Swart, *Physical Review Letters* **116**, 096102 (2016).
- [24] F. J. Giessibl, *Applied Physics Letters* **73**, 3956 (1998).
- [25] F. J. Giessibl, H. Bielefeldt, S. Hembacher, and J. Mannhart, *Applied Surface Science* **140**, 352 (1999).
- [26] J. Welker and F. J. Giessibl, *Science* **336**, 444 (2012).
- [27] A. Biedermann, W. Rupp, M. Schmid, and P. Varga, *Physical Review B* **73**, 165418 (2006).
- [28] N. N. Negulyaev, V. S. Stepanyuk, L. Niebergall, P. Bruno, W. Auwärter, Y. Pennec, G. Jahnz, and J. V. Barth, *Physical Review B* **79**, 195411 (2009).
- [29] J. E. Sader and S. P. Jarvis, *Applied Physics Letters* **84**, 1801 (2004).
- [30] J. E. Sader, B. D. Hughes, F. Huber, and F. J. Giessibl, (2017), arXiv:1709.07571.
- [31] *See Supplemental Material for further experimental details, the tunneling current and the full set of Δf data corresponding to Figs. 1(a) and (b) and their corresponding deconvoluted short-range potentials, a further analysis why the iron adatom hopped only once in Figs. 1(a) and (b), the error analysis in the determination of the absolute tip height, the lateral force profile along a more asymmetric direction, a detailed analysis of the tilt directions of the tips, the simulation based on van der Waals and electrostatic interactions for describing the inverted asymmetry in the lateral force fields, the tunneling current and Δf images of five pentamers created via lateral manipulation using CO tips, the tunneling current versus distance and Δf versus distance curves on a CO molecule before and after building up the pentamer shown in Fig. 3 and the STM and AFM images before and after creating a Si trimer.*
- [32] W. L. Bragg, *The London, Edinburgh, and Dublin Philosophical Magazine and Journal of Science* **28**, 355 (1914).
- [33] M. Schneiderbauer, M. Emmrich, A. J. Weymouth, and F. J. Giessibl, *Physical Review Letters* **112**, 166102 (2014).
- [34] M. Emmrich, M. Schneiderbauer, F. Huber, A. J. Weymouth, N. Okabayashi, and F. J. Giessibl, *Physical Review Letters* **114**, 146101 (2015).
- [35] J. E. Lennard-Jones, *Proceedings of the Physical Society* **43**, 31 (1931).
- [36] C. A. de Coulomb, *Mémoires de l'Académie royale des sciences* **88**, 578 (1788).
- [37] R. Smoluchowski, *Physical Review* **60**, 661 (1941).